

RESEARCH ARTICLE

Modulation Signal Automatic Recognition Technology Combining Truncated Migration Processing and CNN

YAXU XUE¹, (Member, IEEE), YANTAO JIN¹, SHAOPENG CHEN¹,
HAOJIE DU¹, AND GANG SHEN²

¹School of Electrical and Mechanical Engineering, Pingdingshan University, Pingdingshan 467000, China

²School of Computer Science, Hubei University of Technology, Wuhan 430000, China

Corresponding author: Yaxu Xue (yaxu.xue@pdsu.edu.cn)

This work was supported in part by the Project of the Science and Technology Department of Henan Province under Grant 232102211022, Grant 232102221018, Grant 232102240008, Grant 232102240046, and Grant 232102220014; and in part by the National Natural Science Foundation of Hubei under Grant 2023AFB951.

ABSTRACT With the continuous development of wireless technology, automatic modulation recognition plays an increasingly prominent role in military and civilian fields. However, the complex communication environment and diversified strategy bring challenges to modulation signal recognition. Therefore, an automatic modulation signal recognition technique combining truncated migration processing and convolutional neural network is proposed. Then multi-task learning is used to optimize and distinguish easily confused modulated signals. Three datasets, RadioML2016.10A, RadioML2016.10B and RadioML2016.04C are used for experiments. The results show that the modulation signal automatic recognition method proposed in this paper has good recognition accuracy. When the signal-to-noise ratio was 14dB, it reached a maximum of 95.46%. In addition, the Floating Point Operations of the proposed method were 1.71G, the number of parameters was 25636712, and the operation time was 228s, which showed that the method was light in weight and high in calculation efficiency. The optimized recognition technology can effectively distinguish three groups of easily confused signals, and the recognition rate is as high as 100%, and the minimum is not less than 90%. The proposed modulated signal automatic recognition technology has achieved remarkable results in improving the recognition accuracy and processing efficiency, which provides a strong technical support for the development of wireless communication technology, and also provides a new tool for researchers and engineers in related fields.

INDEX TERMS Wireless communication, modulation signal, automatic recognition, truncated migration, convolutional neural network, multi-task learning.

I. INTRODUCTION

In the information age, communication technology has greatly promoted social development and improved all aspects of life. From traditional letters to modern instant messaging, the communication method has witnessed the continuous growth of human demand for information exchange and technological innovation [1]. In this context,

The associate editor coordinating the review of this manuscript and approving it for publication was Chengpeng Hao¹.

wireless communication technology, especially Automatic Modulation Recognition (AMR) technology, has become an indispensable part of the modern communication field [2]. AMR technology exerts a crucial function in various fields. In the military, AMR technology can help intercept and identify enemy communication signals, providing support for intelligence collection and communication interference [3]. In civilian field, especially the promotion of 5G and IoT technologies, AMR technology has played a crucial function in spectrum resource management and signal

recognition [4]. However, the complex communication environment and diversified strategy pose challenges to accurate signal recognition. Faced with the increasing diverse signal types and complex communication environments, traditional manual recognition methods are inadequate [5]. Therefore, researchers are constantly seeking new technological means to optimize the accuracy and efficiency. Artificial intelligence and deep learning technologies provide new possibilities for solving this problem. Especially Convolutional Neural Networks (CNN), due to the outstanding performance in natural language processing, are considered the major tool for solving modulation signal recognition problems [6]. Therefore, a CNN modulation signal automatic recognition technology combining truncated migration processing is proposed. The truncated migration algorithm increases the sampling points extracted by CNN. To address the easily confused signal recognition, the automatic modulation signal recognition technology is optimized based on Multi-Task Learning (MTL). The research aims to improve the recognition accuracy and processing efficiency, thereby providing new ideas for the innovation and application of wireless communication technology.

The contribution of the research is to propose an innovative modulation signal automatic recognition technology. The technology is optimized by combining truncated transfer processing and convolutional neural networks, and using a multi-task learning framework. It can significantly improve the recognition accuracy and processing efficiency of easily confused modulation signals.

The research contains five parts. The first part summarizes the existing research on signal recognition technology. Part two mainly introduces the CNN modulation signal automatic recognition technology combined with truncated migration processing and the recognition optimization method based on MTL. The third part proves the performance and feasibility of the designed modulation signal automatic recognition technology through a series of experiments. The fourth part summarizes the full text. The last part discusses from different angles according to the content of the article and points out the significance of the research.

II. RELATED WORK

In modern communication and information technology, signal recognition technology is an essential branch, which involves extracting, analyzing, and identifying specific signal patterns from complex data streams [7]. With the arrival of the digital economy and continuous investment in technological innovation, signal recognition technology has experienced rapid development, showing broad application prospects [8]. Therefore, scholars from various countries around the world are conducting research on signal recognition technology. Y. Lin et al. addressed the real-time and fine-grained processing of wireless signals in communication systems by converting complex signal wave-forms into contour star images. This method filled the gap of deep learning in signal recognition watershed. It provided an effective image

data format representation for deep statistical information of signals [9]. T. Huynh-The et al. designed a cost-effective CNN for robust automatic modulation classification. Various asymmetric Convolutional Kernels (CKs) were used to simultaneously learn the signal spatiotemporal correlation. Then the jumping connection was used to maintain more initial residual information, thereby improving classification accuracy [10]. W. S. Saif et al. proposed an optical performance modulation format recognition technology ground on the machine learning to address the challenges posed by the conflicts in added user bandwidth and quality of service. It drove the development of ultra-low latency and adaptive autonomous optical networks [11]. A. P. Hermawan et al. proposed an optimized CNN-based automatic modulation strategy to satisfy the high accuracy and short computation time of adaptive encoding and modulation in wireless communication. The network adjusted the CNN layers and introduced a new convolutional layer, thereby improving classification accuracy and effectively reducing computation time [12].

In addition, there are three problems when using CNN in radar pulse modulation recognition: the recognition rate increases with the addition of Signal-to-Noise Ratio (SNR) until saturation, and the inability to prove the impact of increased SNR on the performance improvement of CNN. Therefore, Yu et al. proposed a position score-internal benchmark to solve the first two problems, and a position score-external benchmark to solve the third problem, thereby improving the recognition rate [13]. P. Chu et al. proposed a statistical measure for discrimination and formed feature vectors to address the bottleneck of AMR caused by the coexistence of analog and digital modulation in secondary modulation signals. The support vector machine was applied to perform classification work. This improved the recognition ability of signals containing mixed modulation types [14]. Tunze et al. built a CNN that included deep wise convolutional layers and conventional packet convolutional layers to meet the low complexity and robust modulation recognition requirements, achieving high recognition accuracy while maintaining lightweight [4]. S. Ansari et al. identified modulation schemes in signal detection and received signal demodulation in communication networks, using multi-layer perceptrons for digital modulation recognition. Then, the genetic algorithm was applied to obtain the optimal parameters, significantly improving the accuracy and speed of automatically determining digital modulation types under low SNRs [15]. F. Zhang et al. proposed an auto-encoder-based method to enhance the information interaction between in-phase/orthogonal data channels in AMR. The auto-encoder built by the fully connected layer was used to associate features of in-phase/orthogonal data and obtain interaction features from the middle layer, thus improving the recognition accuracy of the most advanced baseline model [16]. Aiming at the limited number of samples in AMR, Lin et al. proposed a transfer learning model, which used audio signal UrbanSound8K as the source domain for

pre-training and a small number of modulated signal samples as the target domain for fine-tuning, thus improving the classification performance [17].

In summary, AMR has made significant progress in the modern communication and information technology. However, faced with the complex communication environments and diverse modulation methods, traditional methods still have problems such as inadequate signal processing and incomplete CNN feature extraction. Therefore, a CNN modulation signal automatic recognition technology combining truncated migration processing is proposed. The innovation lies in effectively expanding the receptive field of CNN through truncated migration algorithm, improving the ability to capture signal features, and optimizing the recognition performance of easily confused signals by combining MTL method.

III. AUTOMATIC MODULATION SIGNAL RECOGNITION TECHNOLOGY BASED ON CNN

This section first creates a mathematical representation of the signal through signal modeling and sampling quantization. Secondly, a data truncated migration algorithm and Parallel Residual Neural Network (PARNN) are proposed to optimize CNN. Finally, a recognition optimization method based on MTL is proposed to address the identification confusion problem between highly similar modulation signals.

A. MODULATION SIGNAL RECOGNITION METHOD GROUND ON TRUNCATED MIGRATION PROCESSING AND CNN

In high noise environment, it is necessary to choose a modulation format with strong anti-noise ability. For long distance transmission, a modulation format with better error performance is crucial. At the same time, there is a trade-off to be made between bandwidth occupancy and spectral efficiency when choosing a modulation format. More complex modulation formats often provide higher spectral efficiency, but may not be applicable in bandwidth-constrained situations. In addition, in certain environments, such as urban, indoor or multi-path transmission environments, the signal may experience different fading characteristics. These specific factors should be considered when selecting the modulation format. Therefore, it is very important to recognize the modulated signal.

In the research of modulation signal recognition methods, signal modeling is the foundation and prerequisite step of the entire development process [18]. The purpose of signal modeling is to create a mathematical representation to describe and simulate the behavior and characteristics of signals in actual conditions. Meanwhile, signal modeling is also significant to ensuring the accuracy, effectiveness, and reliability of the proposed method [19], [20]. Therefore, the research first completes the signal modeling. In actual communication, the radio signal $y(t)$ is shown in equation (1).

$$y(t) = A(t) e^{j(\omega t + \varphi)} x(t) + n(t) \quad (1)$$

In equation (1), $A(t)$ represents the signal gain. $x(t)$ signifies the modulation signal. $n(t)$ signifies the additive Gaussian white noise. ω and φ represent frequency offset and phase offset, respectively [21]. The received signal is sampled and quantized to make it adaptable and convenient for deep learning. Firstly, if the sampling interval is T_s and the sampling point is l , the accepted discrete time sampling matrix Y_D is shown in equation (2).

$$Y_D = [y_1, y_2, \dots, y_l] \quad (2)$$

In equation (2), y_l signifies the l -th sample point of Y_D . The combination of real and imaginary parts forms a signal data set sample, and the complex form of y_l is displayed in equation (3).

$$y_l = I_l + jQ_l \quad (3)$$

In equation (3), I_l signifies the real part. Q_l represents the imaginary part. j represents an imaginary unit. Therefore, Y_D is further represented in equation (4).

$$Y_D = \begin{bmatrix} I_l \\ Q_l \end{bmatrix} = \begin{bmatrix} I_1, I_2, \dots, I_l \\ Q_1, Q_2, \dots, Q_l \end{bmatrix} \quad (4)$$

Y_D serves as the input for subsequent research methods. However, since CNN typically processes image formats, Y_D is set as three-dimensional data and saved in $(2, l, 1)$ format. Among them, “2” represents the two parts of real and imaginary numbers. “ l ” refers to the number of sampling points, which is also represented as data length. “1” signifies the channel dimension. According to the constructed signal model, signals are composed of sampling points. Therefore, according to the local connections, weight sharing, and pooling operations, the core idea of using CNN to achieve modulation signal recognition is to compare sampling point values. CNN places more emphasis on local input features, that is, a small segment of the sequence data rather than the entire data set. When performing modulation signal recognition, it is difficult to effectively compare the feature values among all sampling points, resulting in the “small receptive field” [22], [23]. Therefore, a data truncated migration algorithm is proposed to pre-process the sampling points. Then the PARNN is designed to extract the features of input samples from both horizontal and vertical directions. The data truncated migration algorithm has 7 steps, as displayed in Figure 1.

From Figure 1, in the data truncated migration algorithm, step 1 reshapes the sampling matrix Y_D of the signal. It means that the Y_D is set to three-dimensional data and the reshaped matrix is set to Y_0 . In step 2, the study sets two parameters, S and T , both of which are positive integers. S represents the distance unit that needs to be moved for each truncation. T represents the number of moves. Step 3 is the most crucial operation in the data truncated migration algorithm. After truncating the distance $1 \times S$ from the right end of the original sampling matrix, it is transferred to the left end of the sampling matrix to obtain matrix Y_1 . It is truncated and transferred based on the matrix Y_{D1} for the second time, with

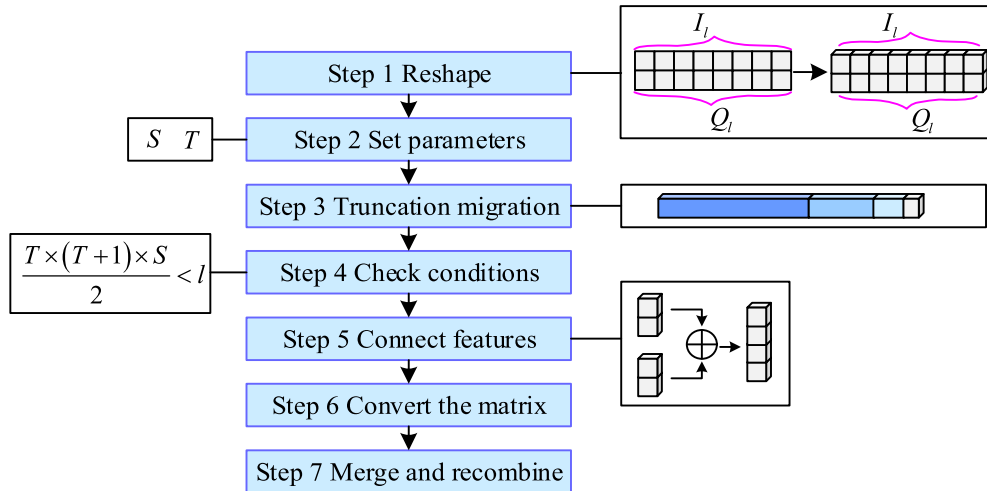


FIGURE 1. Schematic diagram of the data truncated migration algorithm process.

a distance of $2 \times S$, resulting in matrix Y_2 . Similarly, the distance of the T -th truncated transfer is $T \times S$, resulting in matrix Y_T . Step 4 is conditional judgment. After completing T moves, if the condition is met, it is returned to step 3. If it is not met, it proceeds to step 5. The conditional judgment is shown in equation (5).

$$\frac{T \times (T + 1) \times S}{2} < l \quad (5)$$

In step 5, the study uses the ‘‘Concatenate’’ operation to connect all matrices from Y_1 to Y_T to form a new sampling matrix Y'_T . Y'_T is represented by equation (6).

$$Y'_T = Y_0 \oplus Y_1 \oplus \dots \oplus Y_T \quad (6)$$

In equation (6), \oplus represents the ‘‘Concatenate’’ operation. Step 6 converts the new sampling matrix Y'_T into a matrix Y''_T containing amplitude and phase parts, as shown in equation (7).

$$\begin{cases} A = \sqrt{I^2 + Q^2} \\ P = \arctan(I/Q) \end{cases} \quad (7)$$

In equation (7), A represents the amplitude. P represents the phase. I and Q signify the real and imaginary components. Finally, in step 7, the ‘‘Concatenate’’ operation is performed again on Y'_T and Y''_T to obtain the final matrix Y'_D as input. The truncated migration operation in step 3 and the operations in steps 5, 6, and 7 are shown in Figure 2.

In Figure 2, the combination of Y_0 and Y_1 makes the left and right ends of the matrix closer in the horizontal direction, while also making ‘‘ S ’’ and ‘‘ $2S$ ’’ closer in the vertical direction. Similarly, after the feature connection in step 5, CNN can effectively consider all sampling points of the input signal when extracting and comparing local features. After converting the matrix into a matrix composed of amplitude and phase components, it can represent angles and distances. CNN can more effectively extract features and complete modulation signal recognition. After processing the

input signal Y_D using the data truncated migration algorithm, it changes to Y'_D , and its input format also changes from $(2, l, 1)$ to $(2T + 2, l, 2)$. Throughout the process, although the matrix used for the input may be wider in dimension by concatenation operations (because multiple truncated migrated matrices are connected horizontally), this does not mean that the actual duration and length of the signal itself is increased. The total number of sampling points of the signal remains the same, but the order and layout of sampling points have changed. On the basis of input information processing, CNN is improved by adding PARNN. Its network structure is shown in Figure 3.

In Figure 3, Conv signifies the convolutional layer. Pool signifies the max pooling layer. Dense signifies the dense. PARNN contains two convolutional layers. The step size of Conv1 is $(2, 8)$, and the Conv2 is $(4, 4)$. The arrangement of pre-processed sampling points is no longer continuous, but rather on the spatial matrix, which is related to both the horizontal and vertical directions. Therefore, Conv1 and Conv2 can simultaneously focus on the characteristics of the input signal in both horizontal and vertical directions. Subsequently, two Batch Normalization (BN) modules are set up, which normalize the features in both horizontal and vertical directions, enabling the network to learn features more effectively in subsequent layers [5], [24]. Finally, the signal is output through the feature connection and feature addition. The signal output by PARNN serves as the input signal for CNN.

To adapt to the data truncated migration algorithm, the 4-layer CNN for traditional modulation signal recognition is improved. Firstly, the improved CNN introduces a max pooling layer after the second and fourth convolutional layers, effectively reducing parameters and computational complexity while retaining key features. Secondly, the size of the convolutional filter in the original CNN is adjusted from $256@1 \times 3$, $256@2 \times 3$, $80@1 \times 3$, and $80@1 \times 3$ to $256@4 \times 4$, $256@3 \times 3$, $80@3 \times 3$, and $80@3 \times 3$ to

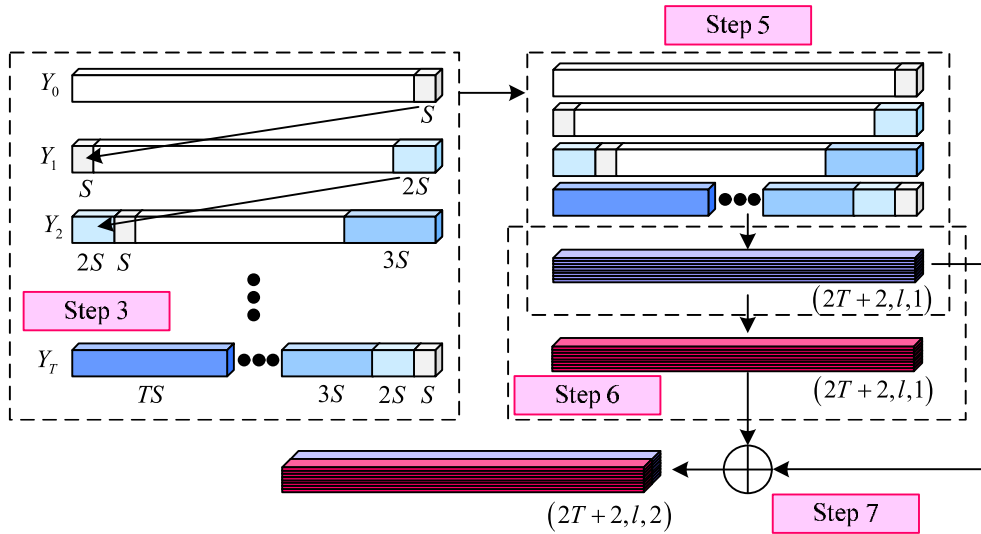


FIGURE 2. Operation diagram of step 3 and steps 5, 6, and 7.

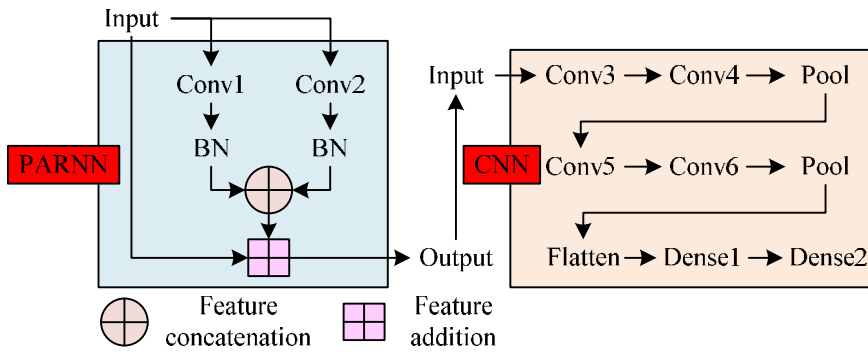


FIGURE 3. CNN structure diagram with the addition of parallel residual neural network.

optimize the feature extraction process. In addition, except for the step size of the first convolutional layer with (2, 1), all other convolutional layers are kept at (1, 1), reducing the model computational complexity while not losing too much spatial information. Finally, the last layer adopts the Softmax for multi-class probability output. Other layers adopt Rectified Linear Unit (ReLU). The ReLU can effectively solve the gradient vanishing and accelerate model training speed. The Softmax is applied to modify the output into a probability distribution, which helps with the classification and recognition of modulated signals.

In addition, an adaptive filter based on signal characteristics is designed, which can dynamically adjust the convolution kernel size according to the SNR and modulation characteristics of the input signal, so as to achieve the optimal trade-off between noise suppression and detail preservation. Further, in order to determine whether the central pixel is damaged, an anomaly detection mechanism based on statistical analysis and machine learning model is introduced [25], [26]. The mechanism can identify central pixels whose characteristics are significantly different from those of surrounding pixels and mark them as potential damage areas, thus improving the accuracy and robustness

of signal recognition. Finally, a trainable attention network is introduced to calculate the importance weights of features, which reflects the correlation between signal features and the current recognition task. Applying these weights to the signal features enables the truncation migration algorithm to pay more attention to the important features and suppress the unimportant ones.

B. OPTIMIZATION METHOD FOR MODULATION SIGNAL RECOGNITION GROUND ON MULTI-TASK LEARNING

The recognition method based on truncated migration processing and CNN can effectively extract signal features and improve recognition accuracy. However, in practical applications, there is high similarity between certain modulation signals, which can lead to confusion during the recognition process, especially in the three sets of signals: Quadrature Phase Shift Keying (QPSK) and 8 Phase Shift Keying (8PSK), 16 Quadrature Amplitude Modulation (QAM16) and 64 Quadrature Amplitude Modulation (QAM64), and Amplitude Modulation-Double Side-band Suppressed Carrier (AM-DSB) and Wide-band Frequency Modulation (WBFM) [27], [28]. Therefore, a modulation signal optimization method combining MTL and 1D

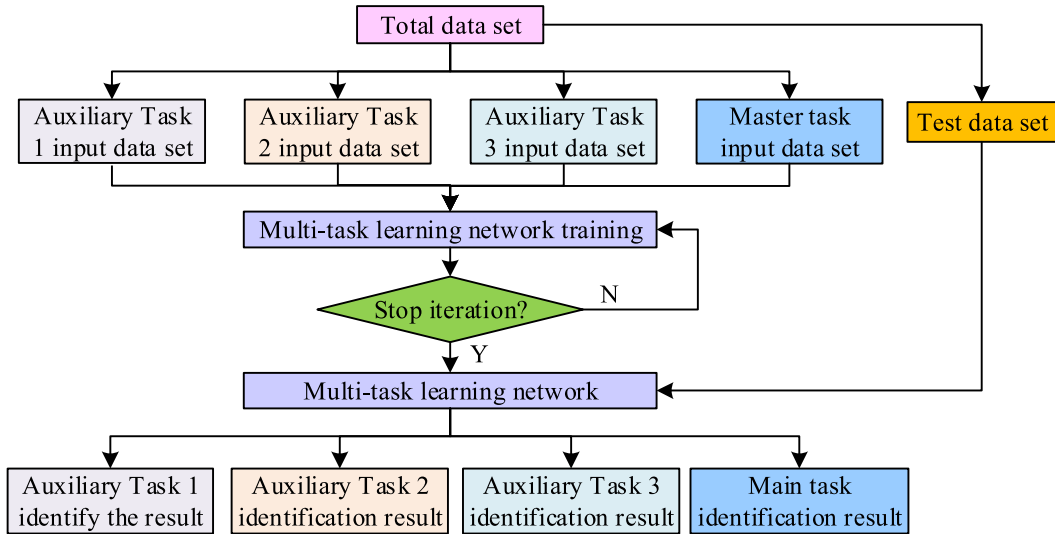


FIGURE 4. The training flow of multi-task learning.

Multi-scale Convolutional Gated Recurrent Unit Network (1DMCG) (MTL-1DMCG) is proposed in this study. MTL is a machine learning paradigm that improves the generalization ability and efficiency of a model by simultaneously learning multiple related tasks. The training process is shown in Figure 4.

In Figure 4, the MTL is different from single task learning. It has multiple inputs and outputs, and tasks are divided into auxiliary tasks and main tasks. Setting auxiliary tasks is to improve the main task. Three auxiliary tasks have been set up for the optimization of modulation signal recognition, namely QPSK and 8PSK, QAM16 and QAM64, AM-DSB and WBFM signal recognition. For each auxiliary task and main task, corresponding input datasets need to be prepared. During the training phase, the network receives input data sets from both auxiliary and main tasks simultaneously. Through the forward propagation, the network outputs the recognition results for each task. Then, through the back-propagation algorithm, the parameters are updated ground on the loss function results. The Cross Entropy Loss is applied as the loss function for auxiliary tasks, as shown in equation (8).

$$L(q, p) = - \sum_{i=1}^C q_i \log(p_i) \quad (8)$$

In equation (8), q represents a true modulation signal category. q_i takes 0 or 1, where 1 indicates belonging to this category. p signifies the predicted probability distribution vector. p_i signifies the probability that the signal is a certain category. C represents the total number of categories. The main task's loss function L_t is the sum of the loss functions of the auxiliary task, as shown in equation (9).

$$L_t = \sum_{i=1}^M \alpha_i L_i \quad (9)$$

In equation (9), α_i signifies the i -th task weight. L_i signifies the loss function of the i -th. M signifies the tasks. After training, the testing set is used to test it and output the recognition results of the auxiliary and the main tasks. Therefore, the network structure of MTL is set up, as shown in Figure 5.

In Figure 5, each auxiliary task adopts a 3-layer Gated Recurrent Unit (GRU) network, which is responsible for extracting temporal features. The features extracted from each auxiliary task are sent to the main task and concatenated with the features extracted from the main task. The main task uses CNN and GRU cascading to build a network. This design simultaneously captures spatial and temporal features. The core of GRU network is gating mechanism, including update and reset gates. The former is shown in equation (10).

$$z_t = \sigma(W_z \cdot [h_{t-1}, x_t] + b_z) \quad (10)$$

In equation (10), z_t signifies the output of the update gate at time t . $\sigma(\cdot)$ signifies the Sigmoid. W_z signifies the weight matrix of the update gate. h_{t-1} signifies the hidden state of the previous time point. x_t represents the current input data. b_z signifies the bias term of the update gate, used to fine tune z_t . The reset gate is shown in equation (11).

$$r_t = \sigma(W_r \cdot [h_{t-1}, x_t] + b_r) \quad (11)$$

In equation (11), r_t represents the output of the update gate. The meaning of other variables is the same as equation (10), except that the object is a reset gate. When identifying phase shift keying signals such as QPSK and 8PSK, the key is to capture the conversion and duration of different phases. The role of update gates and reset gates in GRU is to dynamically adjust the temporal characteristics of signals [29], [30]. After the ‘‘Concatenate’’ operation, the merged feature vectors are then fed into the Dense to learn the complex relationships

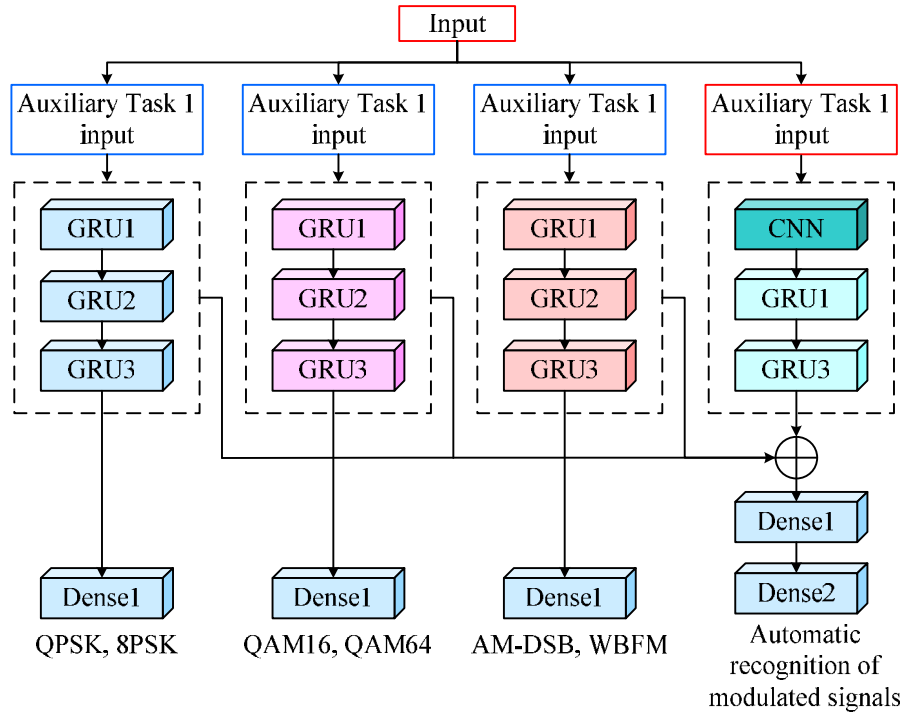


FIGURE 5. Network structure diagram of multi-task learning.

among features, as shown in equation (12).

$$o_i = \phi \left(\sum_{j=1}^n W_{ij}f_j + b_i \right) \quad (12)$$

In equation (12), o_i represents the output of the i -th neuron in the Dense. $\phi(\cdot)$ signifies the activation function. W_{ij} signifies the weight in the i -th and the j -th feature. f_i signifies the i -th feature. b_i represents the bias term of the i -th. In modulation signal recognition, the Dense can identify subtle differences between different modulation types, such as specific modulation characteristics or noise levels of the signal, thereby providing decision-making basis for the output layer [31], [32]. In the main task network, 1DMCG is adopted, with its input being one-dimensional amplitude and phase feature vectors. Figure 6 displays the main task model.

In Figure 6, in the main task model, 1DMCG uses a total of 7 convolutional layers, which utilize CKs with various sizes to extract features from input data. Conv1 uses 64 CKs of size 1, which helps to extract fine-grained features of the signal. Conv2 uses 64 CKs of size 3, which helps capture patterns of medium length. Conv3 uses 64 CKs of size 5 to further capture longer temporal patterns. Conv4 adopts 64 CKs of size 7 to extract larger scale temporal features. Conv5 uses two CKs of size 1, which helps reduce the feature dimensionality while maintaining their diversity. Conv6 uses two CKs of size 1 to further reduce dimensionality. Conv7 uses four CKs of size 1 to decline dimensionality while adding a certain degree of non-linearity. Similarly, in 1DMCG, the feature vectors extracted from different convolutional layers are still concatenated through the ‘‘Concatenate’’ operation to form a longer feature vector,

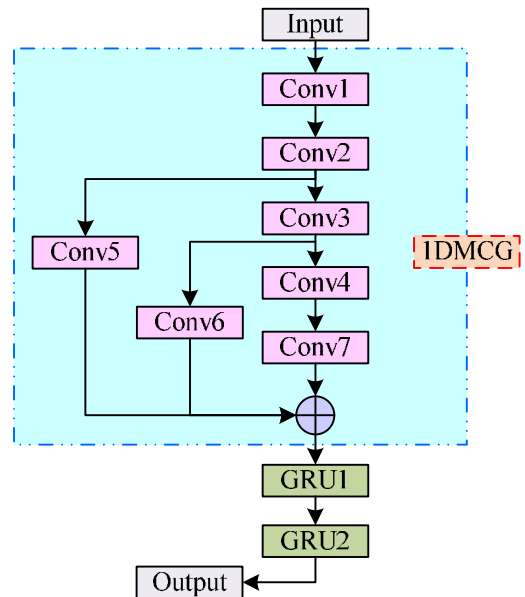


FIGURE 6. Network structure of the main task model.

thereby preserving features of different scales, increasing the model expressive power, and reducing the parameters during the main task model calculation. The GRU network in the main task model has two layers, with the first having 32 hidden units and the second having 16 hidden units.

Overall, the workflow of MTL-1DMCG is as follows. Firstly, multiple auxiliary tasks are set up to enhance the main task performance. The features of the auxiliary and main tasks are extracted through convolutional layers and

GRU networks, and then fused. The cross entropy loss function is applied for optimization. The GRU layer captures temporal features through update and reset gates, while the Dense learns the complex relationships among features. Ultimately, the MTL-1DMCG model can effectively improve its classification ability for modulation signals through this comprehensive method.

IV. PERFORMANCE ANALYSIS OF MODULATION SIGNAL AUTOMATIC RECOGNITION TECHNOLOGY BASED ON CNN

To assess the validity and superiority of the designed modulation signal automatic recognition technology, experiments are conducted on modulation signal recognition methods ground on truncated migration processing and CNN, as well as the method based on MTL. The main content includes experimental environment and parameter configuration, accurate classification performance analysis, etc.

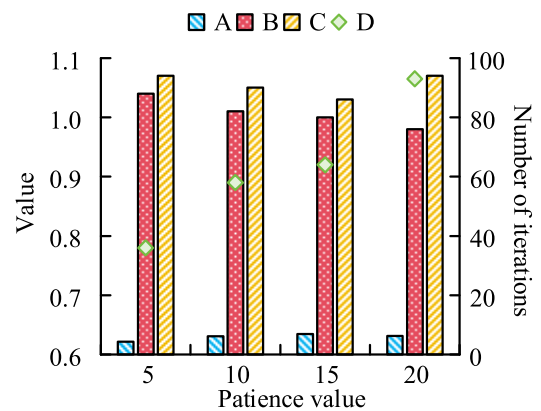
A. PERFORMANCE ANALYSIS OF MODULATION SIGNAL RECOGNITION METHOD GROUND ON TRUNCATED MIGRATION PROCESSING AND CNN

To assess the validity and superiority of the modulation signal recognition method ground on truncated migration processing and CNN. Three data sets RadioML2016.10A, RadioML2016.10B and RadioML2016.04C are used to conduct experiments in this section. RadioML2016.10A, RadioML2016.10B and RadioML2016.04C are three data sets specifically designed for wireless communication signal recognition research, which provide a rich signal sample for the development and testing of AMR technology. These data sets contain signals of different modulation types, each with samples at different SNR levels, which can simulate variable communication environments in the real world [33]. The training to the testing sets is 7:3. The adaptive moment estimation is optimizer. The more detailed experimental configuration and parameter selection are displayed in Table 1.

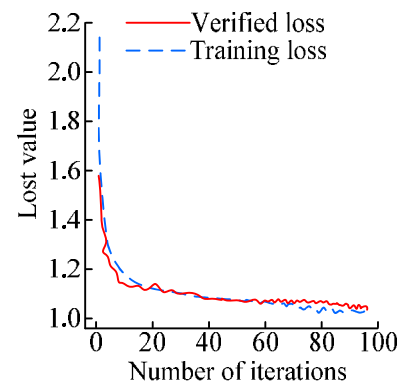
TABLE 1. Experimental configuration and parameter selection.

Experimental configuration		Parameter selection		
Type	Configuration and version	Name	Size	
Hardware	Processor	Intel(R) Core(TM) i7-13700K CPU	Number of iterations	100
	Memory capacity	32.0 GB	Batch size	512
	Graphics card	NVIDIA GeForce RTX 3070ti GPU	Learning rate	0.001
	Operating system	Windows 10	Discard rate	0.5
Software	Language	Python 3.6.10	/	/
	Same device architecture	CUDA 9.0+cuDNN 7.6.5	/	/
	Backend	Tensorflow-gpu 1.9.0	/	/
	Deep learning library	Keras 2.2.4	/	/

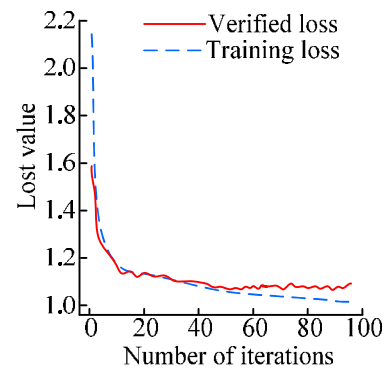
From Table 1, the criteria for selecting parameter values are set according to previous research content and references. The study sets the batch size to 512, which balances the training efficiency and memory consumption. The 100 iterations provide sufficient learning time for the model while avoiding over-fitting. A learning rate of 0.001 was chosen to ensure the stability of the training process. In addition, the random inactivation theory is adopted and the discard rate is set at 0.5. To prevent over-fitting, the study also adds a technique to prevent over-fitting in neural networks, namely the early stop mechanism. The patience value selection in the early stop mechanism is tested, as displayed in Figure 7.



(a) Recognition performance under different patience values



(b) The loss value at 15 patience



(c) The loss value at 20 patience

FIGURE 7. Test results of different patience values in the early stop mechanism.

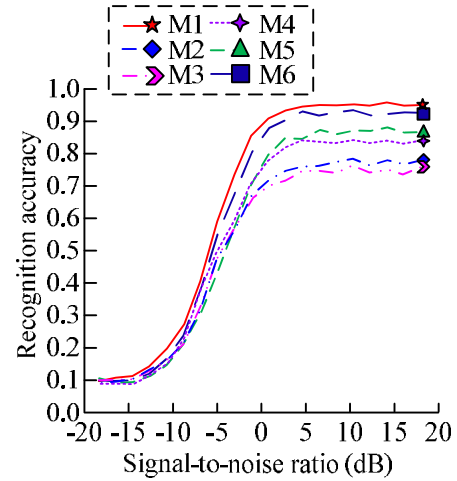
In Figure 7 (a), A, B, C, and D represent the average recognition rate, final loss value, final validation loss value, and iteration number, respectively. In Figure 7 (a), when the patience value was 15, the average recognition rate was the highest, at 63.48%. When the patience value was 20, the final loss value was the lowest, at 0.98. Figures 7 (b) and (c) show the changes in loss values when the patience value was 15 and 20, respectively. In Figure 7 (b), when the patience value was 15, the training loss and validation loss were not significantly different, without over-fitting. In Figure 7 (b), when the patience value was 20, there was a significant difference in the training and the validation losses, with the validation loss reaching 1.07, indicating the over-fitting. Therefore, the patience value was 15. In the data truncation migration algorithm, the parameter S is introduced, which determines the truncation and migration steps and times of the signal sampling matrix, and affects the extraction of signal features. The S value is tested to find the most suitable value. Table 2 displays the results.

TABLE 2. Experimental results of parameter S value.

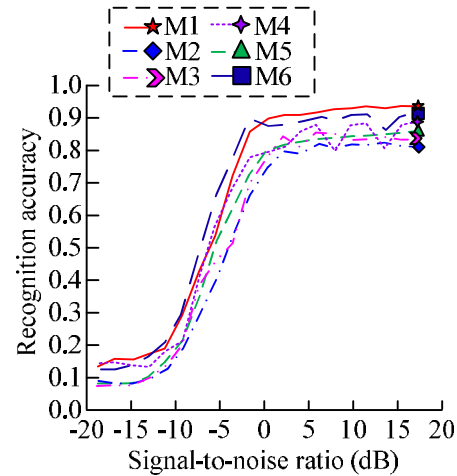
Value	Highest recognition accuracy (%)	Average recognition accuracy (%)	Input shape	One iteration time (s)
1	92.64%	57.46%	(32,128,2)	116
2	92.45%	58.17%	(22,128,2)	86
3	92.98%	61.42%	(18,128,2)	60
4	92.76%	60.33%	(16,128,2)	55
5	91.34%	57.01%	(14,128,2)	53
6	90.28%	55.94%	(12,128,2)	50

According to Table 2, when the S was 3, its highest recognition rate was 92.98%, the average was 61.42%, and the iteration time was 60s. When S took values of 4, 5, and 6 respectively, the iteration time was 55s, 53s, and 50s, which was better than when S took a value of 3. However, the recognition rate was too low, with the highest average recognition rate being only 60.33% and the lowest being 55.94%. Overall, at 60s iteration, the iteration was within the acceptable range. Therefore, when the value of S was 3, it had the highest recognition rate. On the basis of the above content, the modulation signal recognition method ground on truncated migration processing and CNN proposed in the study is compared with five more advanced methods, namely Residual Network (ResNet) method, Complex-Domain Neural Network (CLDNN) method, Inception Network ground on deep learning (Inception), Long Short-Term Memory (LSTM) method, and Multi-Channel Lightweight Deep Neural Network (MCLDNN) method. Six methods are named M1-M6 respectively, with M1 being the designed method. The recognition accuracy results in three data sets is shown in Figure 8.

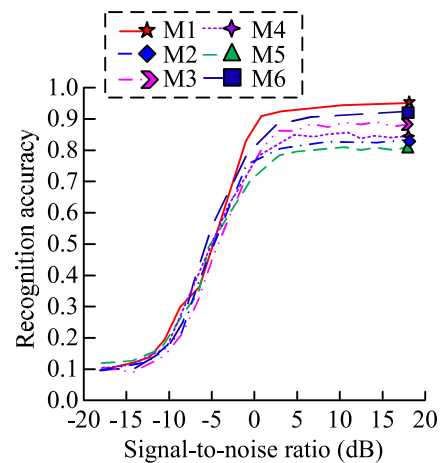
In Figure 8 (a), the recognition accuracy increased with the addition of SNR. The recognition accuracy of M1 was always the highest, reaching the highest at 95.46% when the SNR was 14dB. The M6 ranked second in recognition accuracy, which was an improved method of M2, with an accuracy of 91.27%. The M3 had the lowest recognition



(a) Recognition accuracy of RadioML2016.10A



(b) Recognition accuracy of RadioML2016.10B



(c) Recognition accuracy of RadioML2016.04C

FIGURE 8. Recognition accuracy results and signal recognition confusion moments.

accuracy, which was less than 80%, because it can only extract a single temporal or spatial feature. In Figure 8 (b),

the M6 was slightly higher than that of M1 when the SNR was less than 0, but ultimately M1 had the highest recognition rate. In Figure 8 (c), M1 remained the highest. Overall, the average highest recognition rate of M1 reached 96.08%. This is due to the data truncation and migration algorithm adopted in M1. By increasing the number of sampling points extracted by CNN, the receptive field of the network is expanded, enabling the network to capture signal features more comprehensively. Furthermore, the model complexity is compared and the signal recognition confusion matrix analysis of M1 is conducted, as shown in Figure 9.

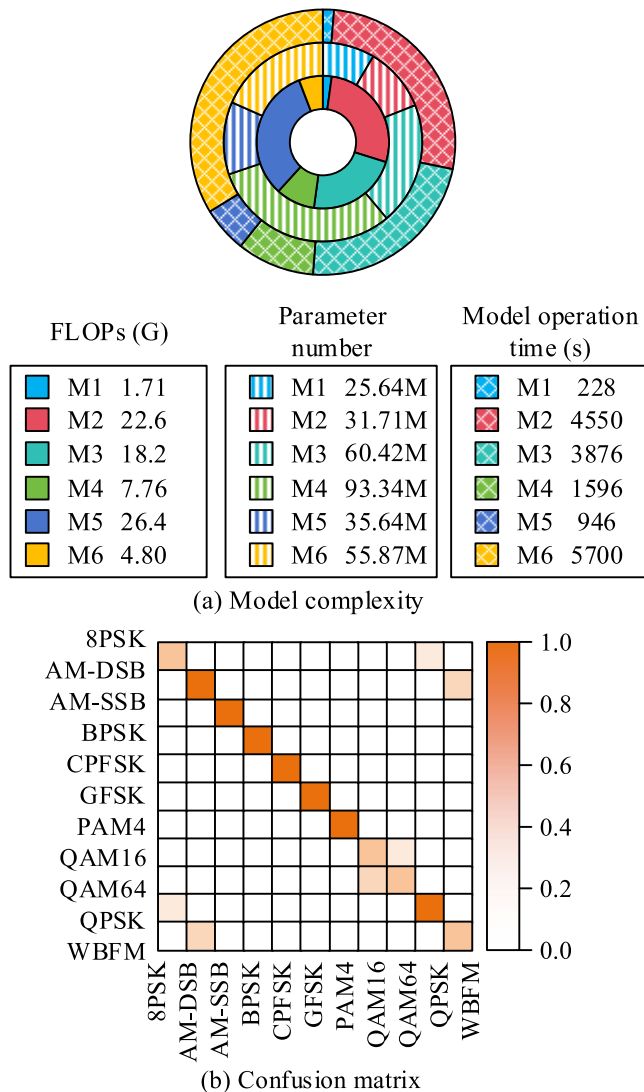


FIGURE 9. Model complexity comparison and confusion matrix.

In Figure 9 (a), the circle represents Floating Point Operations (FLOPs), the number of parameters and the model operation time respectively from the inside to the outside, where the model operation time refers to the time taken for one cycle of model training. As can be seen from Figure 9 (a), research method M1 shows obvious advantages in terms of model complexity and computational

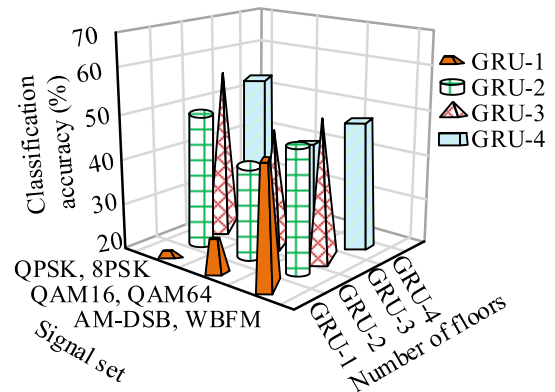


FIGURE 10. Influence of GRU layers on identification results.

requirements. Specifically, the FLOPs of M1 is 1.71G, which is lower than FLOPs of other methods, which means that the model requires less computing resources. At the same time, the number of parameters for M1 is 25,636,712, and fewer parameters not only reduce storage and memory footprint, but also help speed up training and reduce the risk of overfitting. In addition, M1's model operation time is only 228s, showing a short training cycle, which enables the model to iterate quickly, improve training efficiency, and make the model more suitable for real-time applications and online learning. These features are due to the careful optimization design of the CNN model structure, such as the use of smaller convolutional nuclei, the reduction of the number of convolutional layers, the application of effective regularization technology, and the data truncation and migration algorithm to enhance the feature extraction capability. Compared to this, other methods may have shortcomings in these areas, such as requiring more computational resources, longer training times, or higher model complexity. Therefore, M1 not only achieves lightweight design while maintaining high recognition accuracy, but also its fast computing speed and low resource requirements make it suitable for a variety of computing environments, including resource-constrained edge devices, showing great potential in practical applications. According to Figure 9 (b), in the recognition of 11 signals, except for QPSK and 8PSK, QAM16 and QAM64, AM-DSB and WBFM with a recognition rate of about 60%, the recognition accuracy of all other signals was close to 1. The built method can recognize modulated signals, but the recognition success rate was relatively low for very similar QPSK and 8PSK, QAM16 and QAM64, AM-DSB and WBFM signals. In order to further verify the generalization ability of the model in different data sets, the SIGMA-Dataset released by the Fraunhofer Institute of Germany, which contains multiple modulation types of signals and is used for signal recognition and modulation classification research, was further selected for validation of the model [34]. In addition, in the course of training and testing, the channel damage in the real world, such as multipath fading, shadow effect, etc., and adversarial attacks, such as signal injection attacks and interference attacks, are

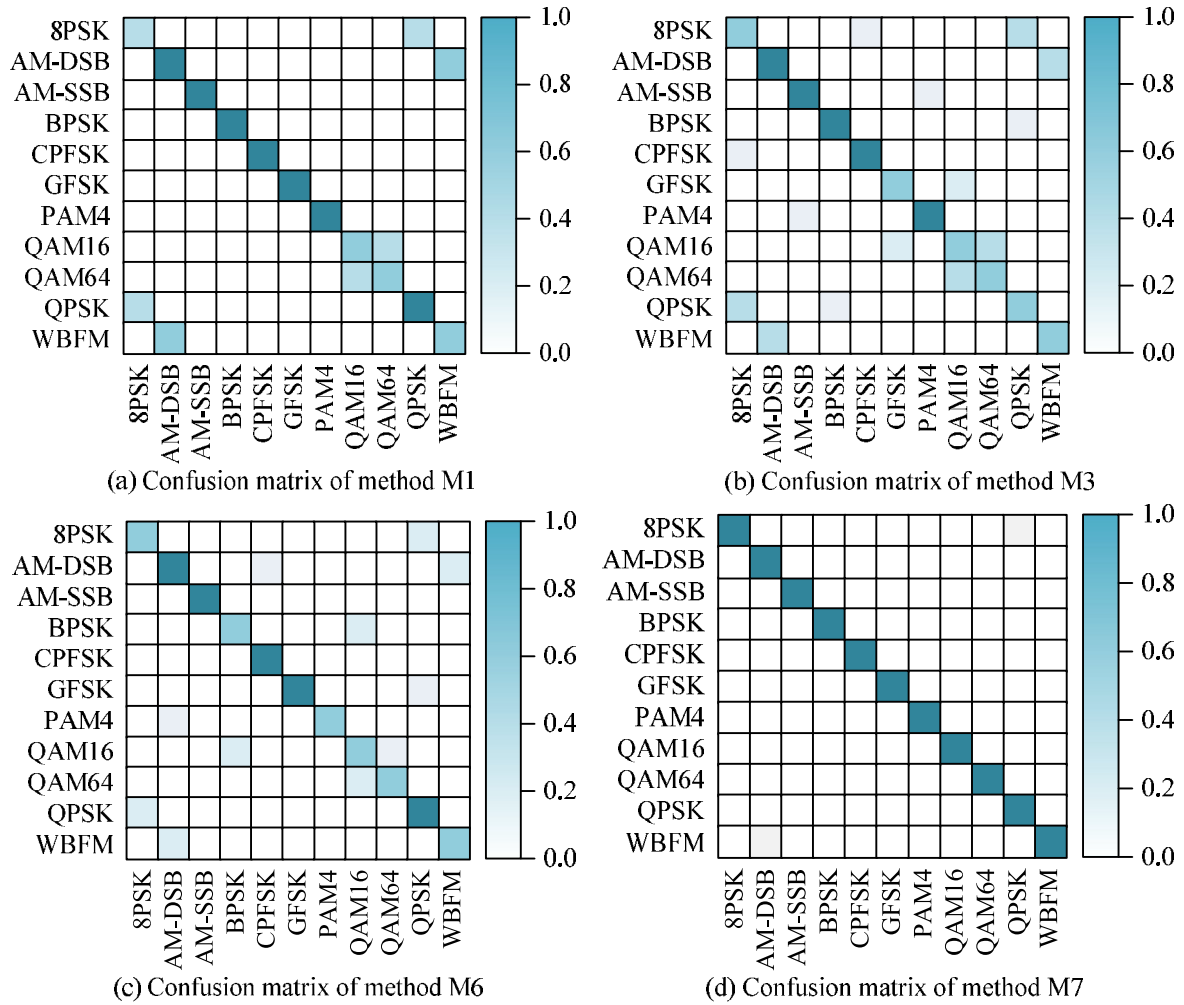


FIGURE 11. Comparative analysis of confusion matrix.

simulated to evaluate the robustness of the model. The results are shown in Table 3.

TABLE 3. Identification accuracy in SIGMA-Dataset.

Method	SNR (dB)				
	-20	-15	-10	-5	0
M1	0.08	0.18	0.21	0.66	0.81
M2	0.04	0.13	0.19	0.59	0.79
M3	0.03	0.14	0.22	0.57	0.80
M4	0.06	0.13	0.18	0.60	0.77
M5	0.02	0.16	0.17	0.64	0.78
M6	0.08	0.14	0.20	0.60	0.74

Method	SNR (dB)			
	5	10	15	20
M1	0.89	0.92	0.94	0.95
M2	0.86	0.91	0.91	0.85
M3	0.82	0.88	0.92	0.90
M4	0.80	0.90	0.90	0.89
M5	0.84	0.92	0.91	0.91
M6	0.82	0.86	0.90	0.89

As can be seen from Table 3, the identification accuracy of research method M1 in SIGMA-Dataset is still the highest, which is similar to the results obtained in RadioML2016.10A, RadioML2016.10B and RadioML2016.04C. However, due

to the existence of channel damage, the overall recognition accuracy has decreased compared with that in three data sets RadioML2016.10A, RadioML2016.10B and RadioML2016.04C, but only by about 1%-2%. This shows that the model has excellent generalization performance and robustness, and can still maintain high recognition accuracy under the condition of external interference.

B. PERFORMANCE ANALYSIS OF MODULATION SIGNAL RECOGNITION OPTIMIZATION METHOD BASED ON MULTI-TASK LEARNING

The effectiveness and superiority of the MTL-1DMCG are validated using three data sets: RadioML2016.10A, RadioML2016.10B, and RadioML2016.04C. The parameter selection adopts the same method as Section III-A, dividing the training and testing sets in an 8:2, with 100 iterations and a batch size of 1024. The optimizer is an adaptive moment estimator, with a learning rate of 0.001. The random inactivation theory is adopted, with a dropout rate of 0.5. Finally, an early stop mechanism is added, with a patience value of 15. Firstly, the GRU layers in the MTL-1DMCG are

analyzed. A 3-layer GRU stack is selected for comparison with other layers. Figure 10 displays the results.

In Figure 10, GRU-1 represents one layer GRU stack. Similarly, GRU-4 represents a 4-layer GRU stack. According to Figure 10, GRU-3 achieved the highest accuracy in the classification of QPSK and 8PSK, QAM16 and QAM64, AM-DSB and WBFM signals, with 52.44%, 43.18%, and 48.13%, respectively. GRU-4 ranked second, with only 49.98%, 39.57%, and 47.14%. This indicates that the selection of 3-layer GRU stack in the study is conducive to improving the recognition rate, possibly because the 3-layer GRU provides a moderate depth, which can not only capture important timing features of signals, but also avoid over-fitting problems that may be caused by excessively deep networks. On this basis, the average recognition accuracy of the MTL-1DMCG is analyzed, as displayed in Table 4.

TABLE 4. Average recognition accuracy of MTL-1DMCG.

Method	SNR (dB)				
	-20	-15	-10	-5	0
M1	0.13	0.17	0.25	0.68	0.82
M2	0.10	0.16	0.24	0.64	0.84
M3	0.12	0.15	0.26	0.62	0.90
M4	0.09	0.15	0.24	0.61	0.85
M5	0.08	0.14	0.22	0.62	0.88
M6	0.09	0.16	0.21	0.64	0.81
M7	0.12	0.17	0.25	0.67	0.92

Method	SNR (dB)			
	5	10	15	20
M1	0.93	0.94	0.96	0.97
M2	0.85	0.87	0.88	0.90
M3	0.91	0.93	0.94	0.95
M4	0.89	0.90	0.92	0.93
M5	0.86	0.87	0.89	0.90
M6	0.82	0.84	0.85	0.87
M7	0.93	0.95	0.97	0.97

In Table 4, M7 represents the MTL-1DMCG model, and M1-M6 represents the method mentioned in the previous section. According to Table 3, there was not much difference between the research method M1 and the MTL-1DMCG model in terms of average recognition rate. The designed method still outperformed other comparative algorithms. Furthermore, the confusion matrix is displayed in Figure 11.

Figure 11 (a) shows the confusion matrix of M1, which is analyzed earlier. Figures 11 (b) and (c) show the confusion matrices of M3 and M6. From Figures 11 (b) and (c), M3 and M6 couldn't distinguish QPSK and 8PSK, QAM16 and QAM64, and AM-DSB and WBFM signals. There were also issues with other signal classification and recognition, such as identifying 4-Level Pulse Amplitude Modulation (PAM4) as AM-DSB. According to the confusion matrix shown in Figure 11 (d), the MTL-1DMCG could significantly improve the recognition rates of three sets of signals: QPSK and 8PSK, QAM16 and QAM64, and AM-DSB and WBFM. Among them, the recognition rates of QPSK and 8PSK, and QAM16 and QAM64 were close to 100%, and the recognition rates of AM-DSB and WBFM were between

90% and 95%. The MTL-1DMCG model performs better in modulation signal recognition tasks mainly because it adopts MTL framework, effective timing feature extraction mechanism, deep feature fusion strategy, optimized network structure selection, appropriate input features and effective regularization technology. These factors together make the MTL-1DMCG model can greatly improve the recognition accuracy when distinguishing easily confused modulated signals. M2, M4, and MTL-1DMCG all select one-dimensional vectors as inputs. Therefore, the recognition rates of M2, M4, and MTL-1DMCG for different input feature vectors are shown in Figure 12.

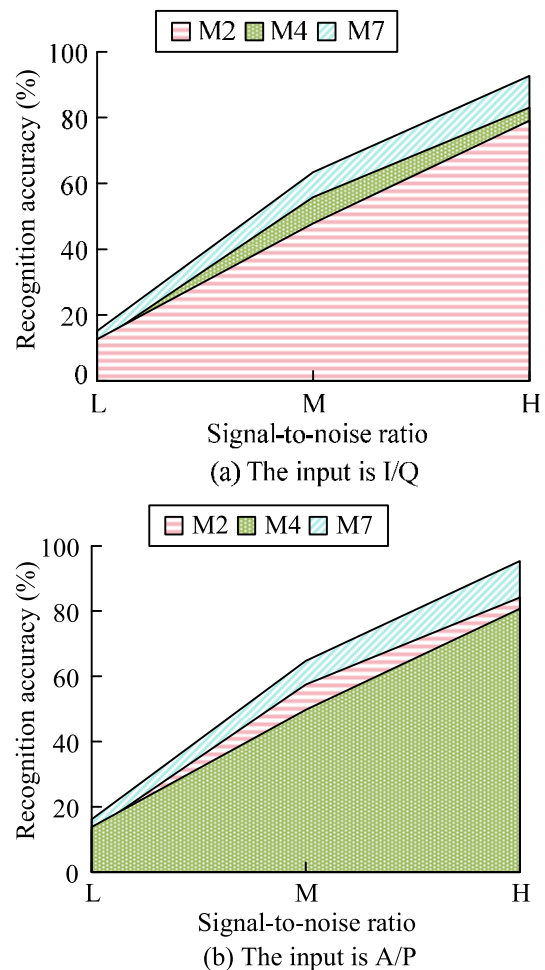


FIGURE 12. Recognition accuracy for different inputs.

In Figure 12, L represents the low SNR range, M represents the medium SNR range, and H represents the high SNR range. In Figure 12 (a), when the input was a feature composed of real and imaginary parts, the recognition accuracy of the MTL-1DMCG in the L, M, and H intervals was 16.76%, 63.18%, and 94.68%, respectively, which was superior to M2 and M4. In Figure 12 (b), when the input was a feature composed of amplitude and phase, the recognition accuracy of the MTL-1DMCG in the L, M, and H intervals was 18.31%, 65.24%, and 97.32%, respectively. This was

not only better than M2 and M4, but also better than the conclusion in Figure 12 (a). This indicates that when amplitude and phase are used as feature vectors for the input signal of the MPL-1DMCG model, it may contain more information to distinguish different modulation types than the real and the imaginary parts. Therefore, the MPL-1DMCG can capture the key features of the signal more effectively, thus improving the recognition accuracy.

V. CONCLUSION

A modulation signal automatic recognition technology based on data truncated migration processing algorithm combined with CNN was proposed to deal with the limitations caused by the complexity of communication environments. To address the identification problem of easily confused signals, MTL and 1DMCG formed the MTL-1DMCG model to optimize the technology. The recognition accuracy of M1 was always the highest, reaching the highest at a SNR of 14dB, which was 95.46%. In addition, the FLOPs of M1 was 1.71G, with a number of parameters of 25636712 and a model operation time of 228s. Compared with other methods, it required the least computational power, the least parameters, and the shortest iteration time, which also had high efficiency and lightweight. In addition, under the optimization of MTL-1DMCG, the average recognition rate reached 96.08%. There was a significant improvement in recognition rate when dealing with highly similar modulation signals like QPSK and 8PSK, QAM16 and QAM64, and AM-DSB and WBFM. Specifically, the recognition rate for QPSK and 8PSK was close to 100%, while the recognition rate for AM-DSB and WBFM was between 90%-95%. The data shows that the data truncated migration processing algorithm effectively expands the receptive field of CNN, and improves the ability to capture signal features and the accuracy. Overall, the modulation signal automatic recognition technology proposed in the study provides new ideas for the innovation and application of wireless communication technology, with broad application prospects and practical value.

VI. DISCUSSION

The proposed modulation signal recognition technology based on truncated migration processing and CNN is in sharp contrast with other state-of-the-art methods in many key performance indicators. For example, in terms of recognition accuracy, the proposed method M1 achieves 95.46% accuracy when the SNR is 14dB, which is not only higher than M2 method based on ResNet, but also higher than M3 method based on CLDNN, M4 method based on Inception network and M5 method based on LSTM. And M6 method of multi-channel lightweight deep neural network MCLDNN. The recognition accuracy of these methods under the same conditions is 91.27%, less than 80%, about 85%, about 85% and about 85%, respectively. In addition, the McL-1dmcg model significantly improves the recognition accuracy of easily confused signals through the multi-task learning framework, such as the recognition rate of QPSK and 8PSK,

QAM16 and QAM64 is close to 100%, while the recognition rate of AM-DSB and WBFM is between 90% and 95%, which is significantly better than other methods. In terms of model complexity, the proposed method M1 has FLOPs of 1.71G, the number of parameters is 25,636,712, and the model operation time is 228 seconds, which shows the characteristics of lightweight and high computing efficiency. In terms of the validity of input features, when the MPL-1DMCG model uses amplitude and phase as input features, the recognition accuracy of low, medium and high SNR ranges is 16.76%, 63.18% and 94.68%, respectively. When the input features are changed to amplitude and phase, The accuracy rate is further improved to 18.31%, 65.24% and 97.32%, which shows the adaptability and robustness of the proposed method to different feature vectors under different SNR conditions. Finally, in terms of generalization ability and robustness, the performance of the proposed method on the SIGMA-Dataset dataset is similar to that of the RadiomL2016 dataset. Even after simulating adduction conditions such as multi-path fading, shadow effect and signal injection attack, the recognition accuracy of the M1 method is only reduced by 1%-2%, which remains at a high level. This further proves the effectiveness and robustness of the proposed method in the actual complex communication environment.

By increasing the number of sampling points extracted by CNN, truncated migration processing algorithm significantly improves the ability to capture signal features. In practical applications, there is a high degree of similarity between some modulated signals, which leads to confusion in the recognition process. As a machine learning paradigm, MTL improves the generalization ability and efficiency of models by learning multiple related tasks simultaneously. Three auxiliary tasks were set up for the recognition of QPSK and 8PSK, QAM16 and QAM64, AM-DSB and WBFM signals. The setting of auxiliary tasks significantly improves the recognition rate of these easily confused signals, which proves the effectiveness of MTL in dealing with similar problems. In the field of wireless communication, especially in resource-constrained environments, lightweight models and high computational efficiency are critical. While maintaining high recognition accuracy, the proposed technology has low FLOPs and the number of parameters, which means that the model can be run on devices with limited computing resources, which is of great significance for practical deployment and application.

It is worth noting that the proposed McL-1dmcg model effectively improves the recognition accuracy of specific modulated signals through the multi-task learning framework. Although the current study focuses on three sets of signals that are easily confused, the flexibility and scalability of the model means that it can be adapted to a wider range of modulation types. If the signal with low classification accuracy is encountered in practice, the model performance can be optimized by customized design auxiliary tasks. In addition, the model's multi-modal feature

extraction and fusion strategy, combined with the spatial feature capture of CNN and the temporal feature analysis of GRU, further enhances its generalization ability. Through continuous model optimization, incremental learning, and feedback loops in actual deployment, the McL-1dmcg model is expected to maintain high accuracy in a wider range of modulation type identification, while cross-domain knowledge and community collaboration will support continuous model improvement.

However, the current research has not addressed the use of deep learning for channel modeling. In addition, although the model is optimized in terms of computational efficiency, its real-time signal processing capabilities in end-to-end systems, including the entire flow of signal acquisition, processing, and classification, have not been deeply explored. At the same time, the possible influence of external hardware defects on recognition accuracy has not been fully considered. Future work will focus on several key directions. Firstly, the channel modeling technology is deeply studied to improve the recognition accuracy of signals in the real communication environment. Second, integrating the signal recognition model into the end-to-end system requires consideration of compatibility and collaboration with other system components. The solution is to develop a modular system design that ensures seamless integration and replacement of signal recognition components, while ensuring efficient management of data and control flows. Finally, the impact of hardware defects on signal recognition performance is evaluated and mitigated.

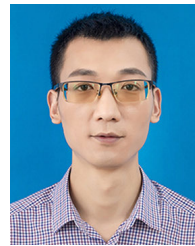
REFERENCES

- [1] Z. Wang, J. Zhang, Z. He, P. Zou, and N. Chi, "Subcarrier index modulation super-Nyquist carrierless amplitude phase modulation for visible light communication systems," *J. Lightw. Technol.*, vol. 39, no. 20, pp. 6420–6433, Oct. 2021, doi: [10.1109/jlt.2021.3099713](https://doi.org/10.1109/jlt.2021.3099713).
- [2] J. N. Njoku, M. E. Morocho-Cayamcela, and W. Lim, "CGDNet: Efficient hybrid deep learning model for robust automatic modulation recognition," *IEEE Netw. Lett.*, vol. 3, no. 2, pp. 47–51, Jun. 2021, doi: [10.1109/LNET.2021.3057637](https://doi.org/10.1109/LNET.2021.3057637).
- [3] N. Jafar, A. Paeiz, and A. Farzaneh, "Automatic modulation classification using modulation fingerprint extraction," *J. Syst. Eng. Electron.*, vol. 32, no. 4, pp. 799–810, Aug. 2021, doi: [10.23919/JSEE.2021.000069](https://doi.org/10.23919/JSEE.2021.000069).
- [4] G. B. Tunze, T. Huynh-The, J.-M. Lee, and D.-S. Kim, "Sparsely connected CNN for efficient automatic modulation recognition," *IEEE Trans. Veh. Technol.*, vol. 69, no. 12, pp. 15557–15568, Dec. 2020, doi: [10.1109/TVT.2020.3042638](https://doi.org/10.1109/TVT.2020.3042638).
- [5] B. Ren, K. C. Teh, H. An, and E. Gunawan, "Automatic modulation recognition of dual-component radar signals using ResSwinT-SwinT network," *IEEE Trans. Aerosp. Electron. Syst.*, vol. 59, no. 5, pp. 6405–6418, May 2023, doi: [10.1109/TAES.2023.3277430](https://doi.org/10.1109/TAES.2023.3277430).
- [6] M. Hu, J. Ma, Z. Yang, J. Wang, and Z. Wu, "Multi-component feature extraction for few-sample automatic modulation classification," *IEEE Commun. Lett.*, vol. 27, no. 11, pp. 3043–3047, Nov. 2023, doi: [10.1109/LCOMM.2023.3318288](https://doi.org/10.1109/LCOMM.2023.3318288).
- [7] S. Wei, Q. Qu, X. Zeng, J. Liang, J. Shi, and X. Zhang, "Self-attention bi-LSTM networks for radar signal modulation recognition," *IEEE Trans. Microw. Theory Techn.*, vol. 69, no. 11, pp. 5160–5172, Nov. 2021, doi: [10.1109/TMTT.2021.3112199](https://doi.org/10.1109/TMTT.2021.3112199).
- [8] Q. Zhou, R. Zhang, J. Mu, H. Zhang, F. Zhang, and X. Jing, "AMCRN: Few-shot learning for automatic modulation classification," *IEEE Commun. Lett.*, vol. 26, no. 3, pp. 542–546, Mar. 2022, doi: [10.1109/LCOMM.2021.3135688](https://doi.org/10.1109/LCOMM.2021.3135688).
- [9] Y. Lin, Y. Tu, Z. Dou, L. Chen, and S. Mao, "Contour stella image and deep learning for signal recognition in the physical layer," *IEEE Trans. Cognit. Commun. Netw.*, vol. 7, no. 1, pp. 34–46, Mar. 2021, doi: [10.1109/TCNN.2020.3024610](https://doi.org/10.1109/TCNN.2020.3024610).
- [10] T. Huynh-The, C.-H. Hua, Q.-V. Pham, and D.-S. Kim, "MCNet: An efficient CNN architecture for robust automatic modulation classification," *IEEE Commun. Lett.*, vol. 24, no. 4, pp. 811–815, Apr. 2020, doi: [10.1109/LCOMM.2020.2968030](https://doi.org/10.1109/LCOMM.2020.2968030).
- [11] W. S. Saif, M. A. Esmail, A. M. Ragheb, T. A. Alshawi, and S. A. Alshebeili, "Machine learning techniques for optical performance monitoring and modulation format identification: A survey," *IEEE Commun. Surveys Tuts.*, vol. 22, no. 4, pp. 2839–2882, 4th Quart., 2020, doi: [10.1109/COMST.2020.3018494](https://doi.org/10.1109/COMST.2020.3018494).
- [12] A. P. Hermawan, R. R. Ginanjar, D.-S. Kim, and J.-M. Lee, "CNN-based automatic modulation classification for beyond 5G communications," *IEEE Commun. Lett.*, vol. 24, no. 5, pp. 1038–1041, May 2020, doi: [10.1109/LCOMM.2020.2970922](https://doi.org/10.1109/LCOMM.2020.2970922).
- [13] Z. Yu, J. Tang, and Z. Wang, "GCPS: A CNN performance evaluation criterion for radar signal intrapulse modulation recognition," *IEEE Commun. Lett.*, vol. 25, no. 7, pp. 2290–2294, Jul. 2021, doi: [10.1109/LCOMM.2021.3070151](https://doi.org/10.1109/LCOMM.2021.3070151).
- [14] P. Chu, L. Xie, C. Dai, and Y. Chen, "Automatic modulation recognition for secondary modulated signals," *IEEE Wireless Commun. Lett.*, vol. 10, no. 5, pp. 962–965, May 2021, doi: [10.1109/LWC.2021.3051803](https://doi.org/10.1109/LWC.2021.3051803).
- [15] S. Ansari, K. A. Alnajjar, M. Saad, S. Abdallah, and A. A. El-Moursy, "Automatic digital modulation recognition based on genetic-algorithm-optimized machine learning models," *IEEE Access*, vol. 10, pp. 50265–50277, 2022, doi: [10.1109/ACCESS.2022.3171909](https://doi.org/10.1109/ACCESS.2022.3171909).
- [16] F. Zhang, C. Luo, J. Xu, and Y. Luo, "An autoencoder-based I/Q channel interaction enhancement method for automatic modulation recognition," *IEEE Trans. Veh. Technol.*, vol. 72, no. 7, pp. 9620–9625, Jul. 2023, doi: [10.1109/TVT.2023.3248625](https://doi.org/10.1109/TVT.2023.3248625).
- [17] W. Lin, D. Hou, J. Huang, L. Li, and Z. Han, "Transfer learning for automatic modulation recognition using a few modulated signal samples," *IEEE Trans. Veh. Technol.*, vol. 72, no. 9, pp. 12391–12395, Sep. 2023, doi: [10.1109/TVT.2023.3267270](https://doi.org/10.1109/TVT.2023.3267270).
- [18] S. Kumar, R. Mahapatra, and A. Singh, "Automatic modulation recognition: An FPGA implementation," *IEEE Commun. Lett.*, vol. 26, no. 9, pp. 2062–2066, Sep. 2022, doi: [10.1109/LCOMM.2022.3184771](https://doi.org/10.1109/LCOMM.2022.3184771).
- [19] H. B. Thameur, I. Dayoub, and W. Hamouda, "USRP RIO-based testbed for real-time blind digital modulation recognition in MIMO systems," *IEEE Commun. Lett.*, vol. 26, no. 10, pp. 2500–2504, Oct. 2022, doi: [10.1109/LCOMM.2022.3191787](https://doi.org/10.1109/LCOMM.2022.3191787).
- [20] S. R. Kshirsagar and T. H. Falk, "Quality-aware bag of modulation spectrum features for robust speech emotion recognition," *IEEE Trans. Affect. Comput.*, vol. 13, no. 4, pp. 1892–1905, Oct. 2022, doi: [10.1109/TAFFC.2022.3188223](https://doi.org/10.1109/TAFFC.2022.3188223).
- [21] B. Jdid, K. Hassan, I. Dayoub, W. H. Lim, and M. Mokayef, "Machine learning based automatic modulation recognition for wireless communications: A comprehensive survey," *IEEE Access*, vol. 9, pp. 57851–57873, 2021, doi: [10.1109/ACCESS.2021.3071801](https://doi.org/10.1109/ACCESS.2021.3071801).
- [22] R. Chakraborty and Y. Hasija, "Predicting MicroRNA sequence using CNN and LSTM stacked in Seq2Seq architecture," *IEEE/ACM Trans. Comput. Biol. Bioinf.*, vol. 17, no. 6, pp. 2183–2188, Nov. 2020, doi: [10.1109/TCBB.2019.2936186](https://doi.org/10.1109/TCBB.2019.2936186).
- [23] H. Sadreazami, M. Bolic, and S. Rajan, "Fall detection using standoff radar-based sensing and deep convolutional neural network," *IEEE Trans. Circuits Syst. II, Exp. Briefs*, vol. 67, no. 1, pp. 197–201, Jan. 2020, doi: [10.1109/TCSII.2019.2904498](https://doi.org/10.1109/TCSII.2019.2904498).
- [24] P. Preethi and H. R. Mamatha, "Region-based convolutional neural network for segmenting text in epigraphical images," *Artif. Intell. Appl.*, vol. 1, no. 2, pp. 119–127, Sep. 2022, doi: [10.47852/bonviewaia2202293](https://doi.org/10.47852/bonviewaia2202293).
- [25] P. Staszewski, M. Jaworski, J. Cao, and L. Rutkowski, "A new approach to descriptors generation for image retrieval by analyzing activations of deep neural network layers," *IEEE Trans. Neural Netw. Learn. Syst.*, vol. 33, no. 12, pp. 7913–7920, Dec. 2022, doi: [10.1109/TNNLS.2021.3084633](https://doi.org/10.1109/TNNLS.2021.3084633).
- [26] S. Lin, Y. Zeng, and Y. Gong, "Learning of time-frequency attention mechanism for automatic modulation recognition," *IEEE Wireless Commun. Lett.*, vol. 11, no. 4, pp. 707–711, Apr. 2022, doi: [10.1109/LWC.2022.3140828](https://doi.org/10.1109/LWC.2022.3140828).
- [27] B. Jdid, W. H. Lim, I. Dayoub, K. Hassan, and M. R. B. Mohamed Juhari, "Robust automatic modulation recognition through joint contribution of hand-crafted and contextual features," *IEEE Access*, vol. 9, pp. 104530–104546, 2021, doi: [10.1109/ACCESS.2021.3099222](https://doi.org/10.1109/ACCESS.2021.3099222).

- [28] I. Yasin, V. Drga, F. Liu, A. Demosthenous, and R. Meddis, "Optimizing speech recognition using a computational model of human hearing: Effect of noise type and efferent time constants," *IEEE Access*, vol. 8, pp. 56711–56719, 2020, doi: [10.1109/ACCESS.2020.2981885](https://doi.org/10.1109/ACCESS.2020.2981885).
- [29] T. A. Almohamad, M. F. M. Salleh, M. N. Mahmud, I. R. Karas, N. S. M. Shah, and S. A. Al-Gailani, "Dual-determination of modulation types and signal-to-noise ratios using 2D-ASIQH features for next generation of wireless communication systems," *IEEE Access*, vol. 9, pp. 25843–25857, 2021, doi: [10.1109/ACCESS.2021.3057242](https://doi.org/10.1109/ACCESS.2021.3057242).
- [30] Y. Lou, R. Wu, J. Li, L. Wang, X. Li, and G. Chen, "A learning convolutional neural network approach for network robustness prediction," *IEEE Trans. Cybern.*, vol. 53, no. 7, pp. 4531–4544, Jul. 2022, doi: [10.1109/TCYB.2022.3207878](https://doi.org/10.1109/TCYB.2022.3207878).
- [31] M. Fetanat, M. Stevens, P. Jain, C. Hayward, E. Meijering, and N. H. Lovell, "Fully Elman neural network: A novel deep recurrent neural network optimized by an improved Harris Hawks algorithm for classification of pulmonary arterial wedge pressure," *IEEE Trans. Biomed. Eng.*, vol. 69, no. 5, pp. 1733–1744, May 2022, doi: [10.1109/TBME.2021.3129459](https://doi.org/10.1109/TBME.2021.3129459).
- [32] C.-F. Teng, C.-Y. Chou, C.-H. Chen, and A.-Y. Wu, "Accumulated polar feature-based deep learning for efficient and lightweight automatic modulation classification with channel compensation mechanism," *IEEE Trans. Veh. Technol.*, vol. 69, no. 12, pp. 15472–15485, Dec. 2020, doi: [10.1109/TVT.2020.3041843](https://doi.org/10.1109/TVT.2020.3041843).
- [33] Z. Liang, M. Tao, J. Xie, X. Yang, and L. Wang, "A radio signal recognition approach based on complex-valued CNN and self-attention mechanism," *IEEE Trans. Cognit. Commun. Netw.*, vol. 8, no. 3, pp. 1358–1373, Sep. 2022, doi: [10.1109/TCCN.2022.3179450](https://doi.org/10.1109/TCCN.2022.3179450).
- [34] B. Hejmanowska, M. Twardowski, and A. Żądło, "An application of the 'traffic lights' idea to crop control in integrated administration control system," *Geomatics Environ. Eng.*, vol. 15, no. 4, pp. 129–152, Oct. 2021, doi: [10.7494/geom.2021.15.4.129](https://doi.org/10.7494/geom.2021.15.4.129).



YAXU XUE (Member, IEEE) received the B.S. degree in electronic information engineering from Xinyang Normal University, Xinyang, China, the M.S. degree in control science and engineering from Chongqing University, Chongqing, China, in 2011, and the Ph.D. degree in traffic information engineering and control from Wuhan University of Technology, Wuhan, China. He is currently an Assistant Professor with the School of Electrical and Mechanical Engineering, Pingdingshan University, Pingdingshan, China. He has authored or co-authored in various journals, such as *IEEE TRANSACTIONS ON COGNITIVE AND DEVELOPMENTAL SYSTEMS*, *IEEE SENSORS JOURNAL*, *IEEE ACCESS*, and *Applied Sciences*. His research interests include hand motion analysis, multi-fingered robotic hand control, machine learning, and signal processing. He is a Reviewer of *IEEE TRANSACTIONS ON CYBERNETICS*, *IEEE TRANSACTIONS ON HUMAN-MACHINE SYSTEMS*, and *IEEE JOURNAL OF BIOMEDICAL AND HEALTH INFORMATICS*.



YANTAO JIN was born in Henan, China, in 1985. He received the B.S. degree in measurement and control technology and instruments specialty from North China University of Water Resources and Electric Power, China, in 2009, and the M.S. degree in test metrology technology and instruments from Hefei University of Technology, Anhui, China, in 2013. From 2013 to 2015, he was with the Electrical Division, Eaton, China, as a Product Engineer. Since 2015, he has been a Teaching Assistant with the School of Electrical and Mechanical Engineering, Pingdingshan University. His research interests include instrument and meter, embedded instrument design, and power system measurement.



SHAOPENG CHEN was born in Henan, China, in 1990. He received the B.S. degree in mechanical design, manufacturing, and automation from Henan University of Science and Technology, China, in 2012, and the M.S. degree in mechatronics engineering from China University of Mining and Technology, Xuzhou, China, in 2016. He is currently a Lecturer with the School of Electrical and Mechanical Engineering, Pingdingshan University, Pingdingshan, China. His research interests include mathematical modeling, optimization algorithm, and signal processing.



HAOJIE DU was born in Henan, China, in 1980. He received the B.S. degree in electronic information engineering from Southwest University, Chongqing, China, in 2005, and the M.S. degree in communication and information systems from Zhengzhou University, Zhengzhou, China, in 2011. He is currently an Assistant Professor with the School of Electrical and Mechanical Engineering, Pingdingshan University, Pingdingshan, China. He is the author of one book and more than five articles. His research interests include machine learning and signal processing.



GANG SHEN received the B.S. degree in electrical automation from Wuhan Institute of Technology, Wuhan, China, in 2002, the M.S. degree in control theory and control engineering from Huazhong University of Science and Technology, Wuhan, in 2009, and the Ph.D. degree in traffic information engineering and control from Wuhan University of Technology, Wuhan, in 2019. He is currently a Lecturer with the School of Computer Science, Hubei University of Technology, Wuhan. His current research interests include cryptography, network security, and privacy preservation.

...